# Novel Beam-Control Techniques Using Dielectric-Image-Line-Fed Microstrip Patch-Antenna Arrays for Millimeter-Wave Applications

Ming-yi Li and Kai Chang, *Fellow, IEEE*

***Abstract*— This paper reports novel beam-control methods which have the potential of low cost and simplicity. The beam direction of the antenna array is controlled by changing the distance between the perturbed dielectric image line (DIL) and a movable reflector plate. A rigorous hybrid-mode theoretical analysis is developed for calculating the dispersion of propagation constants in DIL's without or with the movable reflector plate and, then, for designing beam-control patch-antenna arrays. Experimental results of scanning angles agree well with theoretical predictions at $Ka$-band frequencies.**

***Index Terms*—Beam steering, dielectric image line, millimeter wave, patch antenna.**

## I. Introduction

THE microstrip patch antenna is a good candidate for many applications. It is planar, conformal, easy to fabricate using photolithography techniques, and low cost. The patch antenna can be fed by many methods. One popular method is to feed the patch from a microstrip line through a coupling aperture [1]. For high-frequency applications ($Ka$-band and above), microstrip feed lines have higher conduction losses, and surface modes could also be excited. As a result, the gain of the antenna suffers. To overcome these problems, an aperture-coupled dielectric-image line (DIL) feed was recently proposed as an alternate feed method [2]–[4].

The new beam-control techniques presented in this paper avoid the use of a solid-state or ferrite phase shifters. The techniques are less complicated and expensive as compared to the traditional methods. The electromagnetic (EM) signal travels mainly in the DIL [5], and the propagation constant of the EM field in the DIL can be changed. A movable reflector plate is applied on the back of the DIL feed to form a perturbed structure [perturbed DIL structures with movable reflector plates (DILWRP's)]. The beam direction of the antenna array is controlled by changing the perturbation distance between the DIL and the movable reflector plate. The movement can be controlled mechanically or electromechanically using a motor or piezoelectric material.

The DIL can be analyzed using the effective dielectric constant (EDC) method [5]–[7]. However, the EDC method cannot analyze the DILWRP. To facilitate the design, a rigorous hybrid-mode analysis was developed and used for calculating the dispersion of EM-field propagation constants in DIL structures without or with the movable reflector plate. Angular scans of radiation beams were achieved by changing the perturbation distance of the reflector plate for the DILWRP. Using the theory and design method developed, $Ka$-band microstrip patch-antenna arrays with eight-elements fed by a DIL or DILWRP have been demonstrated with good scanning angles. The arrays also exhibited good impedance matching, high gain, wide-frequency operation, low cross polarization, and low sidelobes.

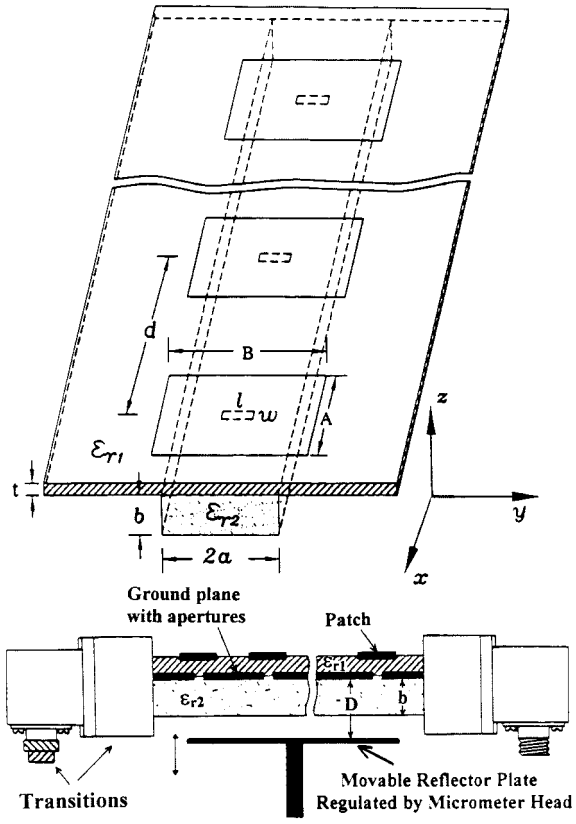


Fig. 1. Aperture-coupled microstrip patch-antenna array fed by DIL. The waveguide components are only used for testing purposes.

## II. Beam-Control Configurations

The structure of aperture-coupled microstrip patch-antenna arrays fed by DIL's is shown in Fig. 1. For testing purposes,

Manuscript received March 20, 1998; revised July 24, 1998. This work was supported in part by the Texas Higher Education Coordinating Board's Advanced Technology Program, by the Energy Resources Program, and by the NASA Lewis Research Center.

The authors are with the Department of Electrical Engineering, Texas A&M University, College Station, TX 77843-3128 USA (e-mail: Chang@ee.tamu.edu).

Publisher Item Identifier S 0018-9480(98)08339-2.

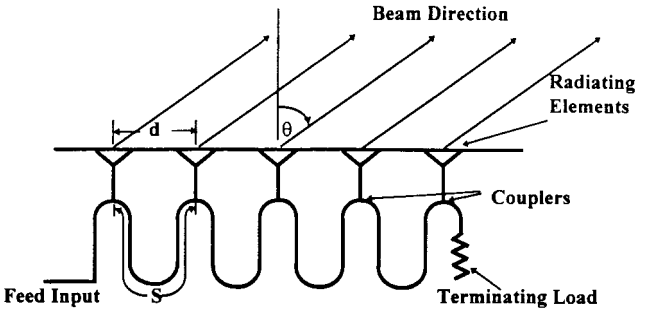


Fig. 2. General schematic diagram of a series-fed beam-steering antenna array.

the signal is coupled to the DIL from the waveguide through transitions. Proper design of DIL dimensions allows single-mode propagation for a considerable range of frequency [5]. For radiating patch elements fed serially along the DIL, there will be a phase delay between elements. This interelement phase delay is linearly progressive and is a function of the propagation constant in the DIL. The radiation-beam angle will be controlled by changing the propagation constant in the DIL. A general schematic diagram of series-fed beam-control antenna arrays is shown in Fig. 2. To form a beam in the direction $\theta$ from broadside, the following equation has to be satisfied [8], [9]:

$$\beta_0 \cdot d \cdot \sin\theta_n = \beta_g \cdot s - 2n\pi \tag{1}$$

where $\theta_n$ is the $n$th beam angle from broadside (normal), $\beta_0 = 2\pi/\lambda_0$ is the free-space propagation constant, $\beta_g = 2\pi/\lambda_g$ is the propagation constant in the DIL feed, $d$ is the distance between radiating elements, $s$ is the length of feed line between elements, and $n$ is the integer. Equation (1) becomes

$$\sin\theta_n = \frac{\lambda_0}{d} \cdot \left(\frac{s}{\lambda_g} - n\right). \tag{2}$$

If $s$ is chosen to be equal to $d$ in the patch-antenna array fed by the DIL, (2) can be written as

$$\sin\theta_n = \lambda_0 \cdot \left(\frac{1}{\lambda_g} - \frac{n}{d}\right). \tag{3}$$

The propagation constants in the DIL can be adjusted and antenna beam angles can be controlled by changing the operating frequency. This is the so-called frequency scanning reported in literature. A method reported here uses a movable metal reflector plate installed in parallel on the back of the DIL feed to form the DILWRP structure. The perturbation spacing between the DIL and the movable reflector plate is varied and controlled precisely using a micrometer head. An accuracy of 1 mil can be reached. The EM field in the DIL is perturbed, and propagation constants and $\lambda_g$ in the DILWRP will change. The radiation beams are scanned at a given operating frequency. The method is simple, low-cost, easy to fabricate, and reliable.

## III. Theoretical Analysis Using Rigorous Hybrid-Mode Method

Accurate computation of $\lambda_g$ is required for theoretically predicting radiation scan angles and for designing beam-control antenna arrays. The EDC method may be used for calculating propagation constants in the DIL, but cannot analyze DILWRP's. It is also not accurate enough in calculating beam-scanning angles due to its approximation.

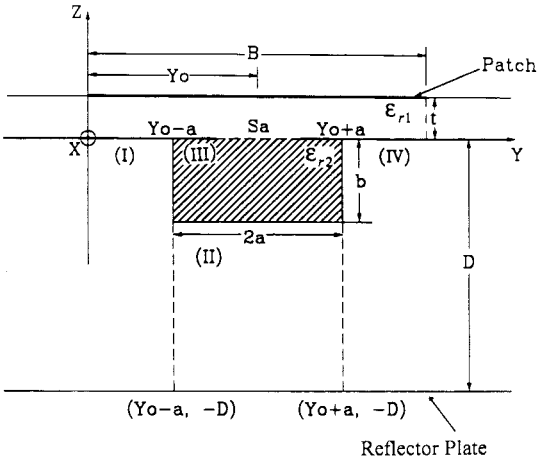


Fig. 3. DILWRP.

A rigorous hybrid-mode analysis [10], [11] was developed and used in this paper for calculating the dispersion of EM-field propagation constants in DIL structures without or with movable reflector plates.

### A. Theory and Formulation

Fig. 3 is the configuration of a DIL of width $2a$, height $b$, and relative dielectric constant $\epsilon_{r2}$. A movable perfect electric reflector plate is placed at a distance $D(z=-D)$ parallel to the ground plane $(z=0)$. The perturbation of the reflector plate on EM-field properties in a DILWRP is adjusted by changing the distance $D$. DILWRP structures will become DIL when $D$ increases to infinity. The cross-section region with a DIL under the ground plane is subdivided into four subregions I–IV. A complete set of field solutions is derived for each sub-area. The dependence of field components on $x$ can be assumed to be an exponential function as $\exp(\pm j\beta_g x)$. $\beta_g$ is the phase propagation constant and is the same in all these four subregions. $y$- and $z$-dependencies of fields in regions I–IV are formulated using eigenfunctions, so that boundary conditions are fulfilled on defined boundaries. All modes are classified as TM and TE with respect to the $z$-direction. Fields in every subregion are expressed in terms of scalar potential functions $\Pi^z$ and $\Lambda^z$, which are for TM and TE to $z$ modes, respectively, as follows:

$$\begin{aligned}
\vec{H}^{\mathrm{TM}} &= \nabla \times (\Pi^z \hat{z}) \\
\vec{E}^{\mathrm{TM}} &= \frac{1}{j\omega\varepsilon_0\varepsilon_r} \nabla \times \vec{H}^{\mathrm{TM}} \qquad (4) \\
\vec{E}^{\mathrm{TE}} &= -\nabla \times (\Lambda^z \hat{z}) \\
\vec{H}^{\mathrm{TE}} &= \frac{-1}{j\omega\mu} \nabla \times \vec{E}^{\mathrm{TE}}. \qquad (5)
\end{aligned}$$

The potential functions can be expressed in Regions I–IV as follows:

*Region I*:

$$\Pi_1^z = \sum_{\nu=0}^{\infty} E_\nu \exp\left[\beta_{y\nu}^{(1)}(y-y_0+a)\right] \cos\left(\beta_{z\nu}^{(1)} z\right) \quad (6a)$$

$$\Lambda_1^z = \sum_{\mu=0}^{\infty} F_\mu \exp\left[\widehat{\beta}_{y\mu}^{(1)}(y-y_0+a)\right] \sin\left(\widehat{\beta}_{z\mu}^{(1)} z\right). \quad (6b)$$

*Regions II and III* ($i=2$ for region II, and $i=3$ for region III):

$$\Pi_i^z = \sum_{\nu=1}^{\infty}\left[A_{i\nu} \sin\left(\beta_{y\nu}^{(i)}(y-y_0)\right) + A'_{i\nu}\cos\left(\beta_{y\nu}^{(i)}(y-y_0)\right)\right] \cdot \cos\left[\beta_{z\nu}^{(i)}(z+D)\right] \quad (7a)$$

$$\Lambda_i^z = \sum_{\mu=1}^{\infty}\left[B_{i\mu} \cos\left(\widehat{\beta}_{y\mu}^{(i)}(y-y_0)\right) + B'_{i\mu}\sin\left(\widehat{\beta}_{y\mu}^{(i)}(y-y_0)\right)\right] \cdot \sin\left[\widehat{\beta}_{z\mu}^{(i)}(z+D)\right]. \quad (7b)$$

*Region IV*:

$$\Pi_4^z = \sum_{\nu=0}^{\infty} G_\nu \exp\left[\beta_{y\nu}^{(4)}(y_0+a-y)\right] \cos\left(\beta_{z\nu}^{(4)} z\right) \quad (8a)$$

$$\Lambda_4^z = \sum_{\mu=0}^{\infty} H_\mu \exp\left[\widehat{\beta}_{y\mu}^{(4)}(y_0+a-y)\right] \sin\left(\widehat{\beta}_{z\mu}^{(4)} z\right) \quad (8b)$$

where $\beta_y^{(k)}$ and $\beta_z^{(k)}$ $(k=1, 2, 3, 4)$ are wavenumbers for TM to $z$ modes; $\widehat{\beta}_y^{(k)}$ and $\widehat{\beta}_z^{(k)}$, corresponding wavenumbers for TE to $z$ modes. Boundary conditions on the plane $z=-b$, $y_0-a \le y \le y_0+a$, between regions II and III, are enforced independently of the remaining conditions. From the continuity conditions for tangential electric and magnetic fields of TM and TE to $z$ modes, $\beta_{y\nu}^{(2)} = \beta_{y\nu}^{(3)} = \beta_{y\nu}$, and $\widehat{\beta}_{y\mu}^{(2)} = \widehat{\beta}_{y\mu}^{(3)} = \widehat{\beta}_{y\mu}$, the following relations are achieved:

$$\beta_{z\nu}^{(2)} \cdot \tan\left[\beta_{z\nu}^{(2)}(b-D)\right] = \frac{\beta_{z\nu}^{(3)}}{\varepsilon_{r2}} \tan\left(\beta_{z\nu}^{(3)} b\right) \quad (9)$$

$$\widehat{\beta}_{z\mu}^{(3)} \cdot \tan\left[\widehat{\beta}_{z\mu}^{(2)}(b-D)\right] = \widehat{\beta}_{z\mu}^{(2)} \cdot \tan\left(\widehat{\beta}_{z\mu}^{(3)} b\right). \quad (10)$$

Wavenumbers $\beta_{z\nu}^{(2)}$, $\beta_{z\nu}^{(3)}$, $\widehat{\beta}_{z\mu}^{(2)}$, and $\widehat{\beta}_{z\mu}^{(3)}$ are real or imaginary in region II, but are purely real in region III. All wavenumbers in the $z$-direction for subregions I–IV can now be solved.

$A_{iv}$, $A'_{iv}$, $B_{i\mu}$, and $B'_{i\mu}$ are unknown constants. The number of equations needed to calculate this eigenvalue problem can be reduced if coefficients $E_m$, $F_m$, $G_m$, and $H_m$ are calculated in terms of $A_{iv}$, $A'_{iv}$, $B_{i\mu}$, and $B'_{i\mu}$. Finally, a complex matrix equation is derived as

$$\begin{bmatrix} M_{1(m,\nu)} & N_{1(m,\nu)} & P_{1(m,\mu)} & Q_{1(m,\mu)} \\ M_{2(m,\nu)} & N_{2(m,\nu)} & P_{2(m,\mu)} & Q_{2(m,\mu)} \\ M_{3(m,\nu)} & N_{3(m,\nu)} & P_{3(m,\mu)} & Q_{3(m,\mu)} \\ M_{4(m,\nu)} & N_{4(m,\nu)} & P_{4(m,\mu)} & Q_{4(m,\mu)} \end{bmatrix} \cdot \begin{bmatrix} A_\nu \\ A'_\nu \\ B_\mu \\ B'_\mu \end{bmatrix} = 0. \quad (11)$$

Matrix elements $M_{k(m,v)}$, $N_{k(m,v)}$, $P_{k(m,\mu)}$, and $Q_{k(m,\mu)}(k=1, 2, 3, 4)$ are functions of frequency $f$, perturbation spacing $D$, image line sizes, dielectric constant $\varepsilon_{r2}$, and propagation constant $\beta_g$. All data, except $\beta_g$, in these matrix elements can be calculated when $f$, $D$, image line sizes, and $\varepsilon_{r2}$ are given. Propagation constants $\beta_g$ in the DILWRP are computed by solving the zeros of the determinant of the whole complex matrix equation (11). The effect of different perturbation distance $D$ on propagation constants $\beta_g$ is then computed exactly. Propagation constants $\beta_g$ in DIL structures are calculated by choosing a very large distance $D$.

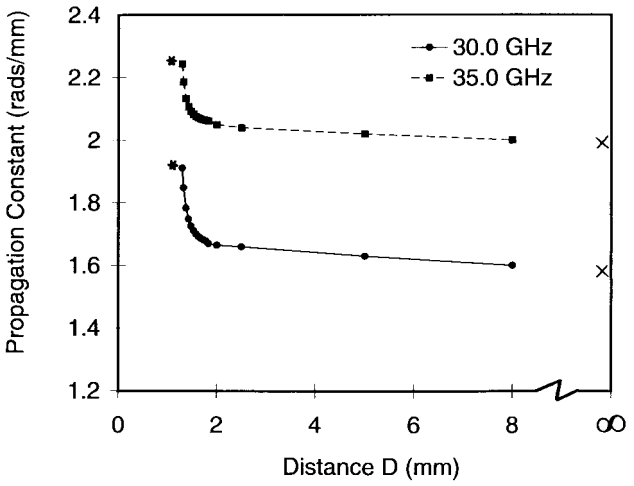


Fig. 4. Computed propagation constants $\beta_g$ for $Ka$-band DILWRP with different distance $D$ at 30.0 and 35.0 GHz. Image line sizes: 1.27 mm × 2.54 mm, $\varepsilon_{r2}=10.5$, $-\bullet-$ 30.0 GHz, $-\blacksquare-$ 35.0 GHz, hybrid-mode analysis, × EDC method, * $H$-guide theory.

### B. Numerical Results

For a given operating frequency and DILWRP structure characteristics, the determinant of the complex matrix in (11) is computed and examined for its zero crossing for $\beta_g$ in the range between $\beta_0$ and $\beta_0\sqrt{\varepsilon_{r2}}$. Propagation constants $\beta_g$ are then determined. The complex double precision is used in calculating the determinant. A full set of real and imaginary $\beta_{zv}^{(2)}$ and $\widehat{\beta}_{z\mu}^{(2)}$ has to be included for computing complex matrix elements in (11). Imaginary $\beta_{zv}^{(2)}$ and $\widehat{\beta}_{z\mu}^{(2)}$ in region II play a very important role in the final matrix determinant calculation. The correct way to choose real and imaginary roots has been studied and found in this paper. A calculation accuracy better than 1.0% and fast convergence are achieved in this paper using only five TE modes and five TM modes, which include four real modes and one imaginary mode.

Propagation constants $\beta_g$ in a DILWRP are found to be different when the perturbation distance $D$ changes. This is useful for the beam-control application. Fig. 4 shows numerical results of $\beta_g$ in a $Ka$-band DILWRP for different distance $D$ at 30.0 and 35.0 GHz. $\beta_g$ is found to increase 15.1% at 30.0 GHz and 9.13% at 35.0 GHz when distance $D$ decreases from 10.0 to 1.3 mm. Two special cases are also considered: $D=\infty$ and $D=b$. The EDC method is an approximate method and can be used only for structures with an infinitive reflector plate distance $D$. The $H$-guide [5] is a special case of a DILWRP when the distance $D$ is equal to the thickness $b$ of the DIL. Calculated results using the EDC method and

$H$-guide theory are also given in Fig. 4 for comparison. For these two special cases, the results indicate that the theory agrees well with the results calculated using the EDC method and $H$-guide theory.

## IV. Beam-Controllable Array Design

Operating frequency range, propagation constants $\beta_g$ in DIL feeds, distance $d$ between radiating patch elements, perturbation spacing $D$, and the effect of different $D$ on $\beta_g$ are several key parameters for designing microstrip patch-antenna arrays fed by DIL's or DILWRP's. These values determine the beam angles of radiation patterns as seen in (1)–(3). Propagation constants $\beta_g$ and its dispersion are determined by the operating frequency, DIL structure characteristics, and the perturbation spacing $D$. Ideally, DIL should be kept as large as possible for millimeter-wave applications, in order to ease fabrication problems and lessen the effects of size variations on the guide wave length and scan angle. At the same time, single-mode operation must be maintained in the propagation of the signal in the DIL with only a single radiation beam from an antenna array. The unit ratio of DIL size of $a/b = 1$ provides the maximum bandwidth [5]. For good field containment and single-mode operation, the following formula can be used to select unit aspect ratio $a/\lambda_0$ for DIL structures:

$$\frac{a}{\lambda_0} \approx \frac{0.32}{\sqrt{\varepsilon_{r2} - 1}}. \tag{12}$$

Relative dielectric constant $\varepsilon_{r2}$ of the DIL should be chosen not too small in order to get enough dispersion in DIL feeds, and then to realize wide scan ranges. $\varepsilon_{r2} = 10.5$ is a good choice from our experience. To obtain the broadside radiation at a given center frequency, (3) shows that the distance $d$ between patch elements must be chosen equal to the guide wavelength. In practice, it is nearly impossible to choose $d = \lambda_g$ due to impedance-match problems of linear-array feed structures. Therefore, the steering angle will not be equal to zero at the center frequency. In this paper, distances $d$ between patch elements are optimized and chosen slightly smaller than $\lambda_g$ at its center operating frequency. Wide-frequency steering ranges and angle scanning ranges are obtained.

The details of the array design have been reported in [4], and can also be found in [12]–[19]. It will not be repeated here.

## V. Experiments and Results

$Ka$-band beam-control microstrip patch-antenna arrays with eight-elements fed by the DIL and DILWRP have been designed, fabricated, and measured. Experimental results are presented and compared with theoretical prediction results.

### A. Dimensions and Characteristics

The rigorous hybrid-mode analysis was used to design the DIL and DILWRP. RT-Duroid material of relative dielectric constant $\varepsilon_{r2} = 10.5$ was used to make the DIL. The DIL had $2a = 3.00$ mm and $b = 1.27$ mm. A movable metal reflector plate was installed in parallel on the back of the DIL to form a DILWRP. A micrometer head was used to precisely control the perturbation distance $D$ to an accuracy of 1 mil. RT-Duroid

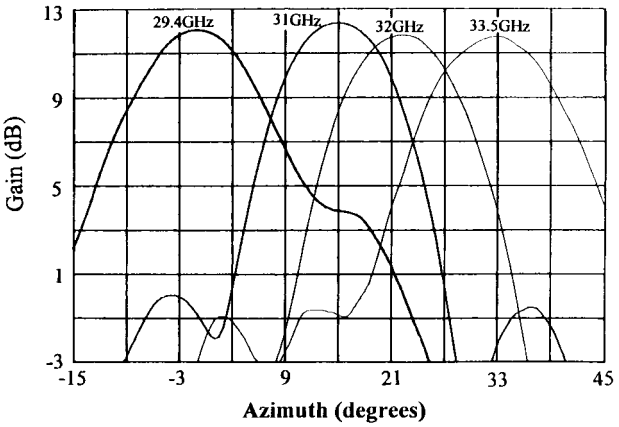


Fig. 5. $Ka$-band frequency beam steering radiation patterns in $E$-plane for eight-element patch-antenna array fed by the DIL at 29.4, 31, 32, and 33.5 GHz.

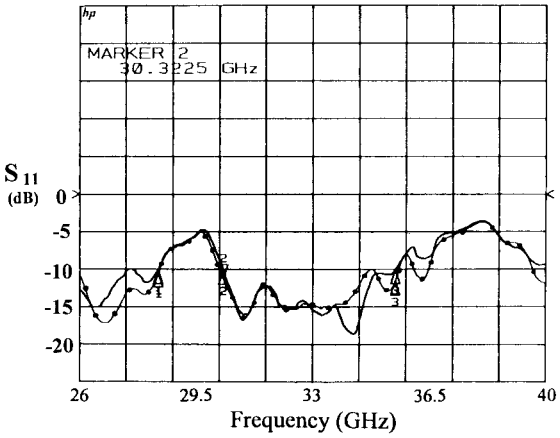


Fig. 6. Return loss of $Ka$-band patch-antenna array for different perturbation distances: —— $(D - b) = 10$ mm, $-\bullet-$ $(D - b) = 1$ mm.

substrate of relative dielectric constant $\varepsilon_{r1} = 2.3$ and thickness $t = 0.764$ mm was used for patches with a radiating length $A = 2.8$ mm and width $B = 3.5$ mm.

Eight-element Dolph–Chebyshev arrays were designed for sidelobes of less than 30 dB. Using the theory developed, the normalized impedances of the elements were determined to achieve the required coupling, and the aperture dimensions were decided. The $Ka$-band arrays were designed with the aperture length $l$ for all eight elements being 2.0 mm. The aperture widths were 0.15, 0.34, 0.47, 0.5, 0.4, 0.29, 0.15, and 0.08 mm from the load. The inter-element distance $d$ was chosen as 5.0 mm.

### B. Performance and Results

The eight-element arrays gave very good performance. They showed good match, high gains, wide operating frequency ranges, large scanning angles, low cross polarization, and low sidelobes. Measurement results of scanning angles agreed well with theoretical predictions.

Patch-antenna arrays fed by the DIL were used to steer the beam by sweeping the operating frequency. The array steered the $E$-plane radiation beams from $-1°$ at 29.4 GHz, 15° at 31 GHz, 22° at 32 GHz, to 33° at 33.55 GHz, as shown in

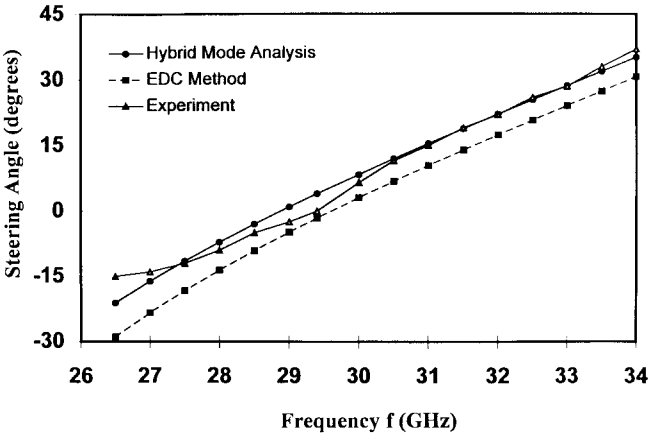


Fig. 7. Beam-steering angles versus operating frequencies for $Ka$-band patch-antenna array fed by the DIL.

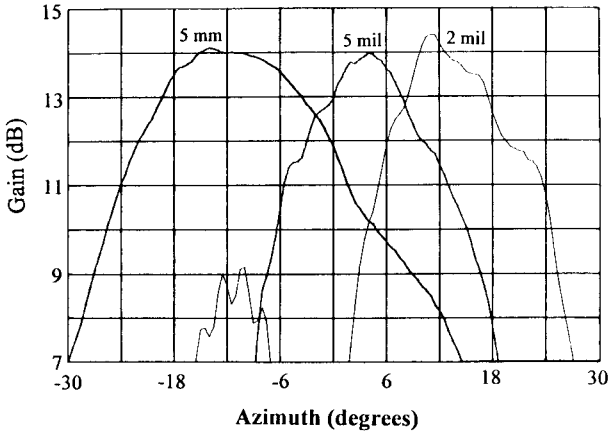


Fig. 8. Beam scanning of $E$-plane radiation patterns for $Ka$-band eight-element patch-antenna array fed by the DILWRP at 28 GHz with different perturbation distances $(D-b)$ of 5 mm, 5 mil, and 2 mil.

Fig. 5. A wide steering angle of 52° in a frequency range of 5.0 GHz was realized. The gains of arrays were found to not change considerably with frequency.

Fig. 6 shows the return loss of the antenna array with a movable reflector plate when the perturbation spacing $(D-b)$ equals 10 and 1 mm, respectively. A good match was found in a wide-frequency range between 30.3 and 35.5 GHz. The return loss was also better than 10 dB below 28.36 GHz. The movable reflector plate did not deteriorate the performance of the antenna array even when the perturbation spacing $(D-b)$ was close to 1 mm. This property makes the antenna array scan in a large angle range when the perturbation distance changes. Fig. 7 gives experimental and theoretical results of beam-steering angles versus operating frequencies for the $Ka$-band eight-element patch-antenna array fed by the DIL. The hybrid-mode analysis and EDC method were used to theoretically compute the steering angles. The predicted results using the hybrid-mode analysis agreed very well with experimental data. Calculation results using the EDC method show less accuracy due to its approximation. An offset was seen in Fig. 7 between experimental results and hybrid-mode analysis in a frequency range from 28.3 to 30.3 GHz. This offset of experimental

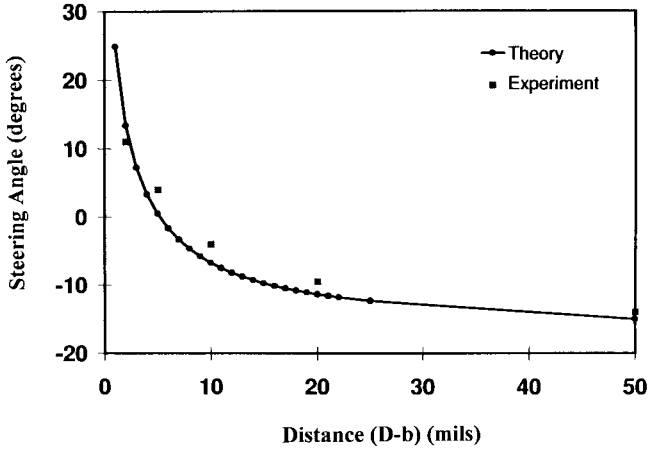


Fig. 9. Beam-steering angles versus perturbation distances for $Ka$-band patch-antenna array fed by the DILWRP at 28 GHz.

results is due to the mismatch of the antenna array in this 2-GHz frequency range, as seen in Fig. 6.

Fig. 8 shows the beam scanning of $E$-plane radiation patterns for different perturbation spacings at the operating frequency of 28 GHz. The main beams were scanned from $-14°$ at $(D-b) = 5$ mm, 4° at 5 mil, to 11° at 2 mil. Gains were found to closely keep the same level. Fig. 9 gives the experimental and theoretical results of beam-scanning angles versus perturbation distances $(D-b)$ for the array fed by the DILWRP. The experimental results agree very well with the theory.

## VI. Conclusions

Novel beam-control techniques using microstrip patch-antenna arrays fed by DIL's have been presented in this paper. Without the reflector plate, the radiation beams of antenna arrays can be steered when the operating frequency sweeps. With the reflector plate, the beam direction of the antenna array can be controlled and scanned by varying the perturbation distance between the DIL and the movable reflector plate at a given operating frequency. The movement can be accomplished mechanically or electromechanically using a motor or piezoelectric materials. A rigorous hybrid-mode analysis has been developed. The theoretical results agree well with the measurements at $Ka$-band frequencies. The techniques provide the advantages of simplicity, low cost, and good performance.

## Acknowledgment

The authors would like to thank Dr. S. Kanamaluru, Dr. J. A. Navarro, Dr. R. Q. Lee, and Dr. A. Zamon for their helpful suggestions and useful discussion.

## References

[1] D. M. Pozar, "A reciprocity method of analysis for printed slot and slot-coupled microstrip antennas," *IEEE Trans. Antennas Propagat.*, vol. AP-34, pp. 1439–1446, Dec. 1986.

[2] M. Y. Li, S. Kanamaluru, and K. Chang, "Aperture coupled beam steering microstrip antenna array fed by dielectric image line," *Electron. Lett.*, vol. 30, pp. 1105–1106, July 1994.

[3] S. Kanamaluru, M. Y. Li, and K. Chang, "Design of aperture coupled microstrip antenna array fed by dielectric image line," *Electron. Lett.*, vol. 31, pp. 843–845, May 1995.
[4] _____, "Analysis and design of aperture coupled microstrip patch antennas and arrays fed by dielectric image line," *IEEE Trans. Antennas Propagat.*, vol. 44, pp. 964–974, July 1996.
[5] P. Bhartia and I. J. Bahl, *Millimeter Wave Engineering and Applications.* New York: Wiley, 1984.
[6] R. M. Knox and P. P. Toulious, "Integrated circuits for the millimeter through optical frequency range," in *Proc. Symp. Submillimeter Waves,* New York, NY, Mar. 1970, pp. 497–516.
[7] T. Itoh and B. Adelseck, "Trapped image guide for millimeter wave circuits," *IEEE Trans. Microwave Theory Tech.,* vol. MTT-28, pp. 1433–1436, Dec. 1980.
[8] A. Hessel, "General characteristics of traveling-wave antennas," in *Antenna Theory: Part 2,* R. E. Collin and F. J. Zucker, Eds. New York: McGraw-Hill, 1969.
[9] R. C. Johnson, *Antenna Engineering Handbook.* New York: McGraw-Hill, Inc., 1993.
[10] K. Solbach, and I. Wolff, "The electromagnetic fields and the phase constants of dielectric image lines," *IEEE Trans. Microwave Theory Tech.,* vol. MTT-26, pp. 266–274, Apr. 1978.
[11] R. Mittra, Y. L. Hou, and V. Jamnejar, "Analysis of open dielectric waveguides using mode-matching technique and variational methods," *IEEE Trans. Microwave Theory Tech.,* vol. MTT-28, pp. 36–43, Jan. 1980.
[12] J. R. James and P. S. Hall, *Handbook of Microstrip Antennas.* Stevenage, U.K.: Peregrinus, 1989.
[13] M. I. Aksun, S. L. Chung, and Y. T. Lo, "On slot-coupled microstrip antennas and their applications to CP operation—Theory and experiment," *IEEE Trans. Antennas Propagat.,* vol. 38, pp. 1224–1230, Aug. 1990.
[14] B. N. Das and K. K. Joshi, "Impedance of a radiating slot in the ground plane of a microstripline," *IEEE Trans. Antennas Propagat.,* vol. AP-30, pp. 922–926, Sept. 1982.
[15] M. D. Pozar and N. K. Das, "Comments on impedance of a radiating slot in the ground plane of a microstripline," *IEEE Trans. Antennas Propagat.,* vol. AP-34, pp. 958–959, July 1986.
[16] S. Kanamaluru, M. Y. Li, and K. Chang, "Simplified analysis of aperture coupled microstrip antenna with image line feed," in *IEEE AP-S Symp. Dig.,* vol. 4, Newport Beach, CA, June 1995, pp. 2098–2101.
[17] C. L. Dolph, "A current distribution for broadside arrays which optimizes the relationship between beamwidth and sidelobe level," *Proc. IRE,* vol. 34, pp. 335–345, June 1946.
[18] T. T. Taylor, "Design of line-source antennas for narrow beamwidth and low side lobes," *IRE Trans. Antennas Propagat.,* vol. AP-3, pp. 16–28, Jan. 1955.
[19] R. J. Mailloux, *Phased Array Antenna Handbook.* Norwood, MA: Artech House, 1994.

**Ming-yi Li** received the B.S. and M.S. degrees in electrical engineering from East China Normal University, Shanghai, China, in 1968 and 1982, respectively.

From 1979 to 1982, he was with the East China Normal University, Shanghai, China, where he was engaged in numerical calculations of EM fields and scattering problems. In 1982, he joined the Shanghai Research Institute of Microwave Technology, Shanghai, China, where he was involved in the research and development of millimeter-wave devices and circuits. This activity resulted in $Ka$-band six-port measurement systems, $Ka$-band attenuators, phase shifters, and $Ka$-band mismatched calibration standard kits. Since 1987, he has been a Research Associate in the Department of Electrical Engineering, Texas A&M University, College Station, where he is involved in research on microwave/millimeter-wave circuits and devices, antennas, power combining, numerical analysis, and microwave measurements. He has published over 50 technical papers in the microwave and millimeter-wave fields.

**Kai Chang** (S'75–M'76–SM'85–F'91) received the B.S.E.E. degree from the National Taiwan University, Taipei, Taiwan, R.O.C., in 1970, the M.S. degree from the State University of New York at Stony Brook, in 1972, and the Ph.D. degree from the University of Michigan at Ann Arbor, in 1976.

From 1972 to 1976, he was with the Microwave Solid-State Circuits Group, Cooley Electronics Laboratory, University of Michigan at Ann Arbor, as a Research Assistant. From 1976 to 1978, he was with Shared Applications, Inc., Ann Arbor, MI, where he worked in computer simulation of microwave circuits and microwave tubes. From 1978 to 1981, he was with the Electron Dynamics Division, Hughes Aircraft Company, Torrance, CA, where he was involved in the research and development of millimeter-wave solid-state devices and circuits, power combiners, oscillators, and transmitters. From 1981 to 1985, he was with TRW Electronics and Defense, Redondo Beach, CA, as a Section Head, where he developed state-of-the-art millimeter-wave integrated circuits and subsystems, including mixers, voltage-controlled oscillators (VCO's), transmitters, amplifiers, modulators, upconverters, switches, multipliers, receivers, and transceivers. In August 1985, he joined the Electrical Engineering Department, Texas A&M University, College Station, as an Associate Professor, and was promoted to a Professor in 1988. In January 1990, he was appointed E-Systems Endowed Professor of Electrical Engineering. He has authored and co-authored *Microwave Solid-State Circuits and Applications* (New York: Wiley, 1994), *Microwave Ring Circuits and Antennas* (New York: Wiley, 1996), and *Integrated Active Antennas and Spatial Power Combining* (New York: Wiley, 1996). He served as the editor of the four-volume *Handbook of Microwave and Optical Components* (New York: Wiley, 1989, 1990). He is the Editor of the *Microwave and Optical Technology Letters* and the Wiley Book Series in Microwave and Optical Engineering. He has published over 300 technical papers and several book chapters in the area of microwave and millimeter-wave devices, circuits, and antennas. His current interests are in microwave and millimeter-wave devices and circuits, microwave integrated circuits, integrated antennas, wide-band and active antennas, phase arrays, microwave power transmission, and microwave optical interactions.

Dr. Chang received the Special Achievement Award from TRW in 1984, the Halliburton Professor Award in 1988, the Distinguished Teaching Award in 1989, the Distinguished Research Award in 1992, and the TEES Fellow Award in 1996 from Texas A&M University.